T-BOLT BEARING STRENGTHS IN COMPOSITE BLADE APPLICATIONS

A J E Ashworth Briggs[1], Z Y Zhang[2*], H N Dhakal[2]

[1]*Designcraft Ltd, Merlin Quay, Hazel Road, Southampton, SO19 7GB*
[2]*Advanced Polymer and Composites (APC) Research Group, School of Engineering, University of Portsmouth, Portsmouth, Hampshire, PO1 3DJ*
**email: zhongyi.zhang@port.ac.uk*

Keywords: Laminate, bearing strength, t-bolt, blade.

Abstract

T-bolts have been extensively used to attach composite blades to rotor hubs in both tidal and wind energy applications. Fitting of t-bolts to the composite component is achieved through the intersection of an in-plane hole with a through plane hole, altering the geometry of the bearing interface. It is important to understand whether this geometry affects the laminates ultimate bearing strength. In this study, monotonic tests were made to measure the ultimate bearing strengths of pin loaded double shear and t-bolt loaded connections for E-glass / Epoxy laminates with a high percentage of reinforcement orientated to the load axis. The internal failure mechanisms at ultimate load are observed by Micro CT. Both fibre matrix shearout and delamination are observed prior to ultimate failure. This study demonstrates that the ultimate bearing strength of t-bolt loaded connection can be 20% lower than an equivalent double shear connection, and that for highly orientated laminates with specific reinforcement architecture the first visible damage occurs at a similar level to the generic Germanischer Lloyd design allowable for load introduction zones. Bearing pressure distribution was determined through radial strain measurement of a ¼ strain gauge array applied below the bearing interface and was found to resemble a Gencoz distribution.

1 Introduction

Composite blade root design presents conflicting geometry requirements for structural and fluid dynamic considerations. Fluid dynamicists seek narrow foil sections, while structural engineers can reliably achieve longer product life spans through increase in blade root diameter. T-bolts and bonded inserts are the most commonly used composite blade connectors (Figure 1) [1]. In T-bolts, load is transferred from the blade to the hub via the bearing interface between the T-bolt and the laminate. Both T-bolts and bonded inserts are susceptible to accelerated hygrothermal degradation of the epoxy adhesive or laminate material at the elevated pressures found at typical installation depths [2] [3].

Pin loaded laminates are reinforced locally with off-axis plies, to withstand local bearing pressure, resulting in a reduction in modulus in the load axis and increase in net tension stress

due to material removal for the pins. Germanischer Lloyd (GL) stipulate a stress threshold within a load introduction zone of 100 MPa.

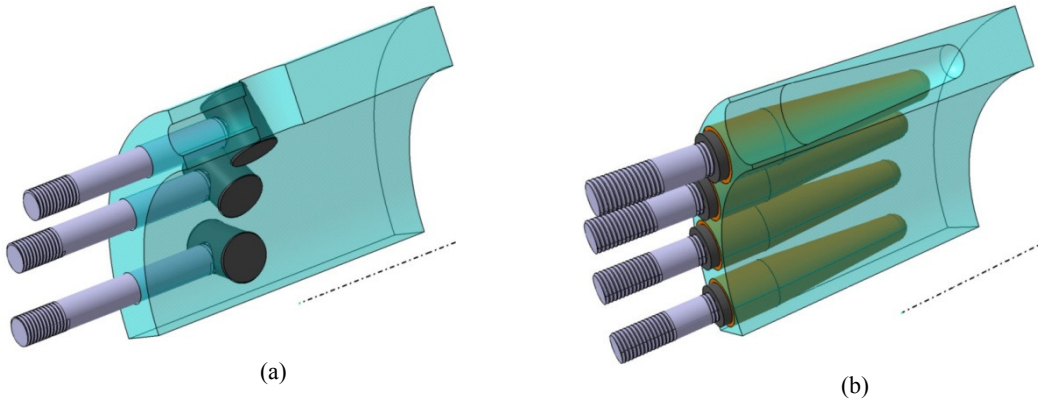

(a) (b)

Figure 1. Common root connectors (a) T-Bolts (b) Bonded inserts

The ultimate strength of a pin loaded joint is affected by laminate isotropy, stacking sequence [4], pin clearance [5-7], lateral constraint [8-10], and the ratio of pin diameter to laminate thickness [11]. The influence of geometry ratios and e/D and W/D has been well documented [12, 13]. Greater e/D ratio is required in T-bolt applications due to the drilling out of material below the barrel nut to provide space for the connecting bolt. This drilling reduces the laminate shear area and bearing area. It is unknown whether the internal geometry affects the ultimate bearing strength of the joint. Some work has shown a limited correlation between Weibull theory and size related strength reduction [15]. Studies investigating size and scale effects have not addressed the impact of materials areal weight variation, on laminates such as those used in the root sections of wind energy blades which often exceed 100mm in thickness.

A joints long term performance is effected by the delamination bearing strength [10] and consequently by the stacking sequence. Placing 90^o plies on the surface of a pin loaded connection can increase the bearing strength by retaining axially loaded plies near the laminate surface [4, 9, 14]. Three dimensional models have been applied to bearing failure. Due to the combination of stresses in a bearing interface where there is an increased probability of delamination in compression and of fibre matrix shear out [16, 17]. The ultimate bearing and delamination resistant strengths of T-bolts does not appear to have been studied. This study aims to determine the ultimate bearing strengths of a t-bolt connection and to compare this with a double shear connection. Good understanding would help to develop design tools and more accurate life prediction for this type of joint.

2 Experimental

2.1 Materials

Laminate was manufactured using Sicomin SR 8100 Epoxy and SD 8731 hardener. A stacking sequence $[(\pm 45,0_3)_n, \pm 45]$ was used. Primary reinforcement was a multi-axial combination mat manufactured from Advantex® Glass by Owens Corning, with 1200 gsm 0^o fibre, combined with nominal 90^o fibre and chopped strand mat (CSM). The resulting laminate consisted of 80% fibre at 0^o, 15% at $\pm 45^o$ and 5% at 90^o orientation.

2.2 Specimen Processing

A $1.5m^2$ panel was laid up, vacuum bagged and infused resulting in a volume fibre of 54%. This was subsequently post-cured according to the manufacturer`s recommendations. Specimens were

cut by water-jet with through thickness holes reamed to a clearance fit of 0.2 mm. In-plane holes were cut using diamond core drills [18].

2.3 Specimen Geometry

The geometry of the specimens is listed in Table 1 and illustrated in Figure. 2.

Series	W	L	e	t	D	d
T-bolt 20	49	210	59.5	20.5	20	12
T-bolt 36	89	360	108	37.5	36	24
Double Shear 20	49	210	59.5	20.5	20	n/a

Table 1. Specimen geometry. Dimensions in mm.

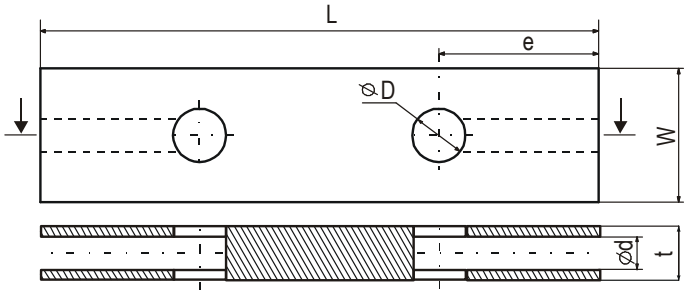

Figure. 2. Specimen geometry plan view and lad axis section

2.4 T-bolt Geometry

A T-bolt assembly is shown in Figure. 3. In practice the tension bolt fails before the laminate ultimate bearing strength is reached [20]. To strengthen the T-bolt assembly, bearing failure loads were estimated from published data [12]. Typical T-bolt geometry based on the ratio of cylindrical nut to tension bolt of 2:1 was altered to 1.67:1 based on preferred size (Table 2).

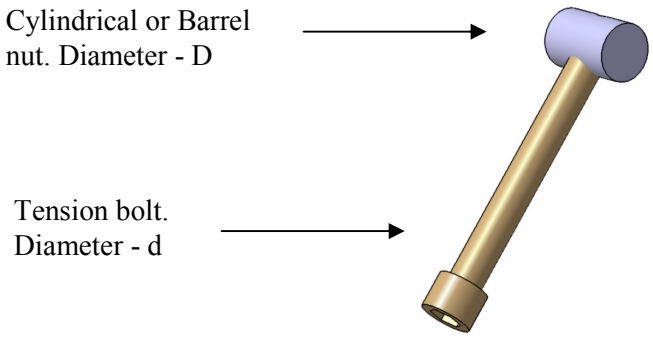

Figure. 3. T-Bolt assembly

Series	D	d	D/d	Grade	Pitch	Yield [kN]	Ultimate[kN]
T-bolt 20	20	10	2	10.9	1.5	52	58
T-bolt 20_{exp}	20	12	1.67	12.9	1.8	92	102

Table 2. Yield and breaking strengths for T-bolt D/d 2:1 and modified experimental T-bolt. Dimensions in mm.

2.5 Monotonic Tests

An ESH 100KN and a Dennison Mayes 630KN machine were used to carry out monotonic tests in accordance with BS EN ISO 14126:1999. Crosshead speed was 1mm per min. Figure. 4 shows the experimental setup for T-bolt and double shear tests.

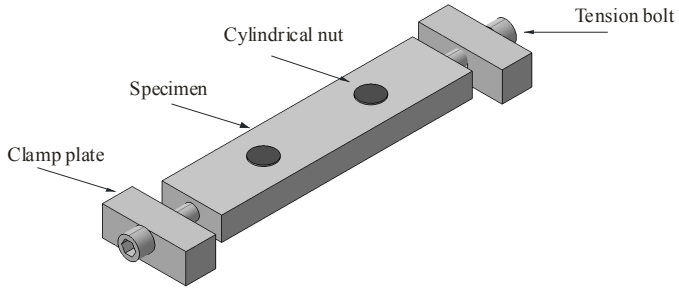

Figure. 4. T-bolted specimen experimental setup

2.6 Radial Strain Measurement

A ¼ radial strain gauge array) was installed, positioned below the bearing interface for the investigation of bearing pressure distribution of a T-bolt connection (Figure. 5). Strain gauge data was recorded using a Vishay Measurements Group System 7000 32 channel data logger installed with Model 7003-8-SG sensor input cards.

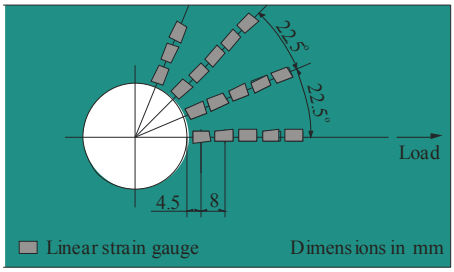

Figure. 5. Layout of ¼ radial strain gauge array.

Investigation was made on damage accumulation below the visible threshold using secondary bending measurement with gauges positioned using AGARD points [22, 23] on opposite laminate faces. It was anticipated that a moment would be developed through the difference in modulus between the mould and bag sides of the laminate due to the effect of compound variability in ply thickness causing waviness in bag face plies.

2.7 Damage Observation

Surface damage accumulation was recorded using video, photography and microscopy. MicroCT analysis was carried out using a Metris XT H 255 255KVa CAT back projection system to inspect specimens for subsurface damage.

3 Results and Discussion

3.1 Ultimate Bearing Failure

The average experimental failure loads presented in Table 3 were obtained from monotonic tests. The bearing strengths were calculated using Eq. (1), (2) & (3) respectively [20].

$$F_{bru} = \frac{P_{ult}}{A_b} \quad (1)$$

$$A_{b\,TB=}\ t.D - \frac{\pi.d^2}{4} \quad (2)$$

$$A_{b=}\ t.D \quad (3)$$

Where F_{bru} is the bearing stress, P_{ult} the ultimate load, t the thickness, D the diameter of the load pin, d the tension bolt diameter, A_b and A_{bTB} the pin joint, and T-bolt bearing areas.

The ultimate bearing strength F_{bru}, is a function of the failure load P_{ult} and A_b. Bearing area was calculated using Eq. (2) & (3), where t is the specimen thickness, D the diameter of the pin or cylindrical nut, and d the diameter of the tension bolt.

Specimen Type	**Failure Load [kN]**	**Bearing Area[mm^2]**	**F_{bru} [MPa]**
T-bolt 20mm	75.5	297	254
Double Shear 20mm	142.9	420	340

Table 3. Experimental failure loads and ultimate bearing strengths

The ultimate bearing strength of the T-bolt connection is 20% lower than the double shear connection (Table 3). The reduction in strength is an indication of the presence of a geometry effect caused by the alteration of the bearing surface geometry on the T-bolt bolt, introducing additional free edges, which might promote edge buckling and delamination.

3.2 Damage Evolution

3.2.1 First non-linearity of load vs. displacement plot

Table 4 presents the bearing stress at the first non-linearity of the load vs. displacement plot where the non-linearity shows a change in laminate modulus which may be attributed to accumulated damage

Specimen Type	**Non-linearity Load [kN]**	**Non-linearity σ_{br} MPa]**
T-bolt 20mm	52	175
Double shear 20mm	119	283

Table 4. Load and bearing strengths at the first non-linearity on load vs. displacement plot.

3.2.2 First visible damage

The first visible damage for a T-bolt specimen was observed at 107 MPa, directly below the cylindrical nut. Initially an opaque spot appeared, which developed into a delamination between a 0^o ply and 90^o fibre bundle (Figure. 6).

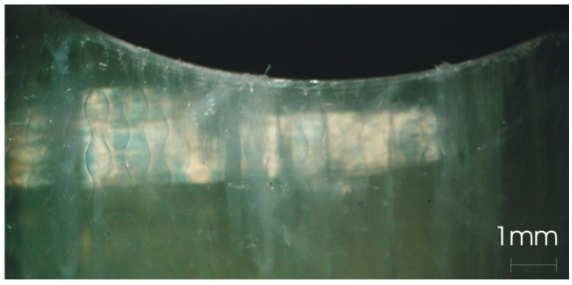

Figure. 6. Microscopy image of a 20mm T-bolt specimen after loading to 107 MPa. Delamination between a 0^o ply and 90^o fibres is visible. The visible edge is the bearing interface and the load applied from the top.

It was not possible to inspect the double shear specimens during testing due to masking of the specimens by the test linkages.

3.2.3 Ultimate failure

Figure 7 presents a microCT image of a 20mm T-bolt specimen loaded to the point of first major loss of stiffness. Inspection of the microCT scans reveals that the laminate in the bearing area is diagonally cracked though 3 of the 0^o axis unidirectional plies. Visually inspection revealed a slight bulging to the external specimen surface, delamination of surface plies along the bearing interface, and a small split in the laminate surface.

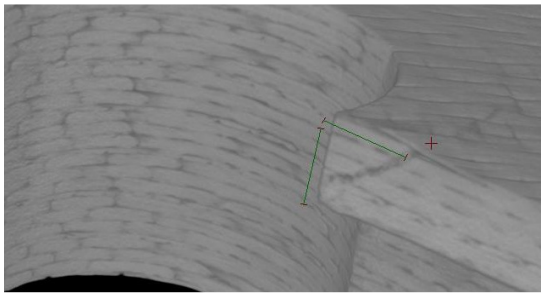

Figure. 7. MicroCT image for specimen 1.2 after loading to 65KN, with the section taken along the load axis. The surface ply is displaced by material which has cracked diagonally below the bearing interface

3.2.4 General Observations

Damage was observed to develop on the moulded surface of each specimen prior to the bag face of the laminate This may attributable to a difference in modulus between the two faces of the laminate. At a bearing stress of 165 MPa, fine white lines were observed below the bearing interface in line with the load axis. These increased in number and length with increase in load.

3.3 Bearing Pressure

Experimental results show a peak radial strain at 22.5^o (Figure. 8 (a)). Figure. 8 (b) shows experimental stress, calculated from the laminates apparent modulus for each change in angle from the load axis. The resulting experimental stress distribution resembles that of a Gencoz pressure distribution (Eq. (4)) [24].

$$\sigma_r = \frac{4P}{\pi dt}\left[cos\Psi - \sum_{n=5.9}^{\infty} \frac{5}{14(n-1)(n-8)}.\cos n\Psi - \sum_{n=3.7}^{\infty} \frac{2}{5(4-n)^2}.\cos n\Psi\right] \quad (4)$$

Where σ_r is the radial stress and Ψ is the angle between the radius and the load axis.

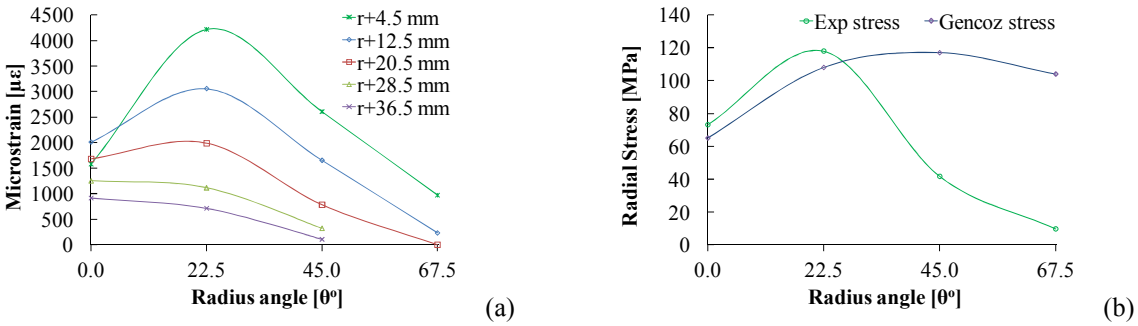

Figure. 8. Experimental strain results for a 36mm T-bolt specimen with pin radius r=18mm, loaded to 85 KN (a) Radial strain (b) Comparison of Experimental and Gencoz radial stress for constant bearing area

The radial strain distribution for isotropic carbon laminates [21] has been shown to resemble a cosine pressure distribution with peak values at 0^o, and decrease in magnitude as the angle between the load axis and radius is increased. Laminates with reinforcement orientation highly biased to the load axis, when combined with a T-bolt connection appear to bear some resemblance to a Gencoz pressure distribution with the region of peak stress no longer aligned with the load axis (Figure. 8 (b)). The radius 22.5^o from the load axis was the where most extensive damage was initiated.

4 Conclusions

The intersecting holes and reduction in laminate thickness of the bearing interface of the T-bolt assembly when compared to a double shear connection effects the bearing properties of the connection.

- T-bolts ultimate bearing strength is reduced by 20%
- For constant e/D and W/D ratios the mode of failure differs becoming less progressive
- Damage accumulation occurs at approximately 36% lower bearing stress
- The radial strain distribution of T-bolt connection in highly orientated orthotropic laminates, differs from that of isotropic pin-loaded laminates. The location of peak strain is 22.5^o from the 0^o axis, similarity is noted to the Gencoz pressure distribution.
- The strength of the metal T-bolt assembly may be increased by altering the ratio of D:d geometry of the, where D is equal to laminate thickness
- The influence of reinforcement architecture on laminate delamination strength remains to be quantified.

Acknowledgements

The authors acknowledge the provision of a Denison Mayes 630KN test machine by the Faculty of Engineering and the Environment at the University of Southampton, and would like to thank Professor Jean-Luc Beney of the La Haute Ecole d'Ingénierie et de Gestion du Canton de Vaud (HEIG-VD), Switzerland for his collaboration and assistance with Catia V.

References

[1] Burton T., Sharpe D., Jenkins N., Bossanyi E. *Wind Energy Handbook*. John Wiley & Sons, Ltd, Chichester (2002).

[2] Zanni-Deffarges M.P., Shanahan M.E.R. Diffusion of water into an epoxy adhesive: comparison between bulk behaviour and adhesive joints. *International Journal of Adhesion and Adhesives*, **15**, pp. 137-142 (1995).

[3] Pilli S.P., Simmons K.L., Holbery J.D., Shutthanandan V., Stickler P.B., Smith L.V. A novel accelerated moisture absorption test and characterization. *Composites Part A: Applied Science and Manufacturing*, **40**, pp. 1501-1505 (2009).

[4] Aktas A., Dirikolu M.H. The effect of stacking sequence of carbon epoxy composite laminates on pinned-joint strength. *Composite Structures*, **62**, pp. 107-111 (2003).

[5] Liyong T. Bearing failure of composite bolted joints with non-uniform bolt-to-washer clearance. *Composites Part A: Applied Science and Manufacturing*, **31**, pp. 609-615 (2003).

[6] Kelly G., Hallström S. Bearing strength of carbon fibre/epoxy laminates: effects of bolt-hole clearance. *Composites Part B: Engineering*, **35**, pp. 331-343 (2004).

[7] McCarthy M.A., Lawlor V.P., Stanley W.F., McCarthy C.T. Bolt-hole clearance effects and strength criteria in single-bolt, single-lap, composite bolted joints. *Composites Science and Technology*, **62**, pp. 1415-1431 (2002).

[8] Khashaba U.A., Sallam H.E.M., Al-Shorbagy A.E., Seif M.A. Effect of washer size and tightening torque on the performance of bolted joints in composite structures. *Composite Structures*, **73**, pp. 310-317 (2006).
[9] Sun H-T., Chang F-K., Qing X. The Response of Composite Joints with Bolt-Clamping Loads, Part II: Model Verification. *Journal of Composite Materials*, **36**, pp. 69-92 (2002).
[10] Heung-Joon P. Effects of stacking sequence and clamping force on the bearing strengths of mechanically fastened joints in composite laminates. *Composite Structures*, **53**, pp. 213-221. (2001).
[11] Liu D., Raju B.B., You J. Thickness Effects on Pinned Joints for Composites. *Journal of Composite Materials*, **33**, pp. 2-21 (1999).
[12] Sayman O., Siyahkoc R., Sen F., Ozcan R. Experimental Determination of Bearing Strength in Fiber Reinforced Laminated Composite Bolted Joints under Preload. *Journal of Reinforced Plastics and Composites*, **26**, pp. 1051-1063 (2007).
[13] Okutan B., Aslan Z.l., Karakuzu R. A study of the effects of various geometric parameters on the failure strength of pin-loaded woven-glass-fiber reinforced epoxy laminate. *Composites Science and Technology*, **61**, pp. 1491-1497 (2001).
[14] Yan Y., Wen W.D., Chang F.K., Shyprykevich P. Experimental study on clamping effects on the tensile strength of composite plates with a bolt-filled hole. *Composites Part A: Applied Science and Manufacturing*, **30**, pp. 1215-1229 (1999).
[15] Hou L., Liu D. Size Effects and Thickness Constraints in Composite Joints. *Journal of Composite Materials*, **37**, pp. 1921-1938 (2003).
[16] Camanho P.P., Matthews F.L. Stress analysis and strength prediction of mechanically fastened joints in FRP: a review. *Composites Part A: Applied Science and Manufacturing*, **28**, pp. 529-547 (1997).
[17] Tserpes K.I., Labeas G., Papanikos P., Kermanidis T. Strength prediction of bolted joints in graphite/epoxy composite laminates. *Composites Part B: Engineering*, **33**, pp. 521-529 (2002).
[18] Hocheng H., Tsao C.C. Effects of special drill bits on drilling-induced delamination of composite materials. *International Journal of Machine Tools and Manufacture*, **46**, pp. 1403-1416 (2006).
[19] Hocheng H., Tsao C.C. Comprehensive analysis of delamination in drilling of composite materials with various drill bits. *Journal of Materials Processing Technology*, **140**, pp. 335-339 (2003).
[20] Martínez V., Güemes A., Trias D., Blanco N. Numerical and experimental analysis of stresses and failure in T-bolt joints. *Composite Structures*, **93**, pp. 2636-2645 (2011).
[21] Ireman T., Ranvik T., Eriksson I. On damage development in mechanically fastened composite laminates. *Composite Structures*, **49**, pp. 151-171 (2000).
[22] AGARD Report No 721. *Fatigue Rated Fastener Systems* (1985).
[23] Ekh J., Schön J., Melin L.G. Secondary bending in multi fastener, composite-to-aluminium single shear lap joints. *Composites Part B: Engineering*, **36**, pp. 195-208 (2005).
[24] Gencoz O., Goranson U.G., Merrill R.R. Application of finite element analysis techniques for predicting crack propagation in lugs. *International Journal of Fatigue*, **2**, pp.121-129 (1980).